On the optical anisotropy of conjugated polymer thin films

M. Campoy-Quiles,[1,*] P. G. Etchegoin,[2,†] and D. D. C. Bradley[1,‡]
[1]*The Blackett Laboratory, Imperial College London, Prince Consort Road, London SW7 2BW, United Kingdom*
[2]*The McDiarmid Institute for Advanced Materials and Nanotechnology, School of Chemical and Physical Sciences, Victoria University of Wellington, PO Box 600, Wellington, New Zealand*
(Received 1 February 2005; published 14 July 2005)

In this paper the problem of optical anisotropies in conjugated polymer thin films is revisited and the results in the literature are critically reappraised. Several models for upper bounds on the different types of anisotropies are developed and these are compared with experiment. We analyze both in-plane/out-of-plane and in-plane anisotropies in spin coated and oriented films, respectively. For the in-plane/out-of-plane anisotropy in spin coated films we study the reasons for the large disparity amongst the results reported in the literature, and propose the method of interference enhancement variable angle spectroscopic ellipsometry to retrieve this anisotropy more accurately. Experimental results are reported for poly(9,9-dihexyl fluorene) (spin coated), poly(9,9-dioctylfluorene) (both spin coated and uniaxially aligned), and poly(9,9-dioctylfluorene-co-benzothiadiazole) (both spin coated and uniaxially aligned). Our results concerning the measurement of optical anisotropy can be applied equally well to other molecular systems, such as self-assembled monolayers or Langmuir–Blodgett films.

DOI: 10.1103/PhysRevB.72.045209 PACS number(s): 78.66.Qn, 07.60.Fs, 78.20.Fm

I. INTRODUCTION AND OVERVIEW

This paper seeks to address thoroughly an issue which has been the subject of intense discussion in the conjugated polymer (CP) thin films literature, namely the presence (or otherwise) of optical anisotropies and their physical origin. In particular, we focus on ellipsometry measurements and their modeling and physical interpretation.

Our experience is that in many situations ellipsometric data fits lead to small standard deviations with a low correlation among the parameters for isotropic thin film models.[1] The thicknesses deduced by these fits are in good agreement with those obtained using surface profilometry, and the calculated absorption spectra using the isotropic optical constants match those measured by spectrophotometry. In polyfluorenes, like poly(9,9-dioctylfluorene) (PFO) for example, results for the refractive index also agree with transmission interference fringe measurements, a technique that uses a completely different principle to reflection ellipsometry. Each of these crosschecks gives confidence in the deduced optical constants obtained from isotropic fits. At this level of analysis, the addition of uniaxial anisotropy in the fitting process, as often assumed in the literature, is found to be unnecessary. However, there are good physical reasons why we can expect out-of-plane anisotropies to occur. The main aim of this paper is to study the reasons for this apparent discrepancy: Are there large optical anisotropies in thin CP films? And if they do exist, how do we measure them using ellipsometry?

By refractive index anisotropy, Δn, we mean the difference between the ordinary and extraordinary indices, i.e., $\Delta n = n_o - n_e$ in the transparency region. We can compare the results for polymers with typical values for inorganic crystals like calcite ($CaCO_3$) with $\Delta n \sim 0.172$, and rutile with $\Delta n \sim 0.287$ ($\lambda = 589.3$ nm).[2] Organic crystals of small molecules have anisotropies that range from $\Delta n \sim 0.05$ (Ref. 3) to 0.5,[4] while nonconjugated liquid crystalline polymers have values of $\Delta n \sim 0.04$ (Ref. 5) up to 0.3.[6] Estimates of the anisotropy of low dimensional systems have also been made. Langmuir–Blodgett films of Cd and Pb salts of acetylenic acid were found to have $\Delta n \sim 0.02$.[7] In contrast, very large anisotropies ($\Delta n \sim 1.3-2.4$.) have been recently calculated for carbon nanotubes.[8] The anisotropy of inorganic crystals is usually due to a polarization dependent band gap, while organic systems often have different oscillator strengths in different directions due to particular molecular ordering of transition dipoles.

Initially, isotropic models were used for CP thin films, including polyacetylene[9] and polythiophene.[10,11] In 1995, McBranch *et al.*[12] deduced the presence of a small ($\Delta n = n_{in\text{-}plane} - n_{out\text{-}of\text{-}plane} < 0.08$) anisotropy for two PPV derivatives that they assigned to preferential alignment of the polymer chains in a plane parallel to the substrate surface. This was in agreement with earlier work by Prest and Luca for saturated polymer thin films.[13,14] An interpretation in terms of preferential molecular ordering was generally accepted and anisotropic values for Δn have been widely reported for CPs: They vary drastically from publication to publication. For MEH-PPV Δn values as small as 0.08 (Ref. 12) and as large as 0.7 (Ref. 15) can be found. Typical values, however, are in the range $0.08 < \Delta n < 0.3$. Koynov *et al.* assigned these differences to different molecular weights;[16] they also suggested that the optical constants of MEH-PPV do not depend on the film thickness. However, Zhokhavets *et al.* have shown that the optical anisotropy of P3OT films increases as the film thickness decreases.[17] It is more likely that a combination of molecular weight, film thickness, thermal treatment, and particular chemical structure effects is crucial to understand the wide range of values reported in the literature.

Preferential alignment is sometimes attributed as being a consequence of spin coating (centripetal forces), but this is inconsistent with systematic studies of the anisotropy. The

TABLE I. Review of optical anisotropy data for conjugated polymer thin film samples. A comparison of the refractive anisotropy $\Delta n = n_{in\text{-}plane} - n_{out\text{-}of\text{-}plane}$ can be readily made. Materials are classified as derivatives of PPV, polyfluorenes, and other CPs. The techniques used to measure n are near normal reflectivity, polarized transmission (T) and reflection (R), waveguide modes, transmission VASE, reflection VASE, and SE. These techniques are also listed.

Optical constants of CPs: Review					
Material	Reference, year	Technique	Δn	λ[a] (nm)	Thickness (nm)
PPV derivatives					
PPV	63, 1996	(Near normal R)	n_{TE} only	UV–Vis	33
BCHA-PPV	12, 1995	(Polarized	0.08	514.5	30–60
”	”	T and R)	0.06	488	”
”	”	”	–0.07	457.9	”
MEH-PPV	”	”	0.08	514.5	”
”	”	”	–0.01	488	”
”	”	”	–0.19	457.9	”
MEH-PPV	15, 2000	Waveguiding	0.7	550	210
”	”	”	0.3	580→660	”
MEH-PPV	18, 2002	VASE[b]	0.3→0.2	600→1200	100–150
MEH-PPV	16, 2004	(Near normal R+prism coupling)	0.005→0.2	Transparent	
BuEH-PPV	19, 1999	VASE[b]	0.3→0.2	520→600	~100
OC1C10-PPV	22, 2002	$T\&R$ VASE[c]	0.4→0.2	600→900	~100
Au:MH-PPV	64, 2004	SE	Isotropic	UV-Vis	1100
Polyfluorene homo- and co-polymers					
PFO	65, 2001	(Polarized T +interference fringes)	Isotropic	UV-Vis	~1000
PFO	1, 2005	VASE[d]	Isotropic	UV-Vis	30–200
PF 2/6	26, 2004	VASE[e]	<0.5	550→1000	~50
F8BT	22, 2002	$T\&R$ VASE[c]	0.2→0.15	600→900	133
F8BT	1, 2005	VASE[d]	Isotropic	UV-Vis	650
PFB	23, 2003	$T\&R$ VASE[c]	~0.06	500→900	75
TFB	23, 2003	$T\&R$ VASE[c]	~0.05	500→900	115
PFO copolymer	66, 2000	Grazing angle	0.2	600	
Other CPs					
P3HT	11, 1992	SE[f]	Isotropic	UV-Vis	16.3
P3OT	25, 2004	VASE[b]	~0.12	~810	~80
PEDOT:PSS	24, 2002	VASE+T[b]	0.1→0.4	300→900	40–180
Polysilane derivative	67, 2003	SE[g]	Isotropic	UV-Vis	~40
5 Polyarylene derivatives	68, 2003	SE[g]	Isotropic	UV-Vis	~150
”	20, 2003	VASE[g]	~0.1	Transparent	~150
mLPPP	21, 1997	VASE[d]	~0.03	Transparent	22–133

[a]λ is the measurement at which Δn is quoted: Transparent signifies wavelengths far from the lowest lying absorption peak. UV-Vis signifies the ultraviolet-visible spectrum.
[b]VASE with rotating analyzer (by J.A. Woollam).
[c]Variable angle reflection and transmission rotating-compensator ellipsometry (by J.A. Woollam).
[d]VASE with rotating polariser (by SOPRA).
[e]VASE with multiple substrate analysis.
[f]SE with rotating analyzer.
[g]Phase modulated spectroscopic ellipsometer (by JY Horiba, UVISEL).

anisotropy of P3OT films was found to be independent of spin coating conditions (speed and time), only depending on thickness.[17] Also, drop cast films can be more anisotropic than spin coated ones, suggesting that polymer chains may have a natural tendency for alignment when subjected to particular boundary conditions.

Table I summarizes a representative set of data from the CP literature. A number of important conclusions can be drawn therefrom.

First, the thin film CP values for Δn typically vary from 0 (isotropic) to ~ 0.4; This excludes inconsistent values, such as negative Δn (Ref. 12) or extremely large values (~ 0.7).[15] Second, there is no clear correlation between the film thickness and Δn, but values for PPV derivatives are generally larger than those for polyfluorenes. Third, many techniques suggest anisotropic Δn values. An equivalent number of techniques deduce isotropic values. Fourth, comparing ellipsometric results, it is clear that anisotropic values have been deduced using both rotating polariser units and modulation ellipsometers. $\Delta n \neq 0$ values are thus found using different ellipsometric techniques.

It is interesting to note that, although $\Delta n \neq 0$ values have been reported using variable angle of incidence spectroscopic ellipsometry (VASE),[18–21] it has also been shown that reflection VASE leads to a high correlation among fitting parameters and, therefore, n_e values are not very reliable.[22] Combinations of techniques like transmission and reflection VASE,[22,23] reflection VASE and variable angle transmission,[24] or multiple sample analysis[25] have, accordingly, been employed. Lyons and Monkman[26] have recently carried out a comparison of the optical constants of aligned and unaligned thin polyfluorene films. They described such films as uniaxial with the optical axis perpendicular to the substrate plane or along the chain direction for spin coated and thermotropically aligned films, respectively. Their study was based on point-by-point calculations of the optical constants, followed by a parametric description of the dielectric functions in terms of a superposition of Gaussians. Their results are broadly speaking in agreement with those presented below. It has been shown, however, that the use of parametric fits based on multiple Gaussians or Lorentzians can be greatly improved by the use of optical critical points (as explained later), thus having transitions with a more physical meaning.[1,10] We shall come back to this issue in Sec. III: The results in Table I provide the background for a detailed discussion.

In this paper we first analyze the two main sources of optical anisotropy in thin films, the electromagnetic boundary conditions (TE and TM modes), and the material anisotropy, and hence, estimate an upper limit for Δn for several CPs. We then explore the sensitivity limitations for VASE with a rotating polarizer. Finally, we show how the effects of Δn can be enhanced by the choice of particular substrates for which interference effects can be brought into play. We use this modified technique to deduce Δn for spin coated PFO and aligned films of PFO and poly(9,9-dioctylfluorene-co-benzothiadiazole) (F8BT), considering both the in-plane/out-of-plane anisotropy in spin coated films (the most controversial) and the in-plane anisotropy in oriented films. We note that the results concerning the measurement of uniaxial optical anisotropy presented here are general for uniaxial thin films with a large in-plane component of the dielectric function. Therefore, our main conclusions could be applied not just to conjugated polymer thin films but to other uniaxial thin films, including inorganic crystalline thin films, self-assembled monolayers or Langmuir–Blodgett films.

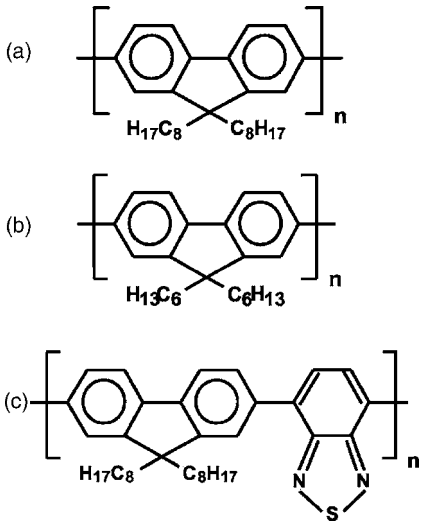

FIG. 1. Chemical structures of (a) PFO, (b) F6, and (c) F8BT.

II. EXPERIMENTAL SECTION

The polymers studied here namely, PFO, poly(9,9-dihexylfluorene) [F6], and F8BT (see chemical structures in Fig. 1), were supplied by The Dow Chemical Company and had been subjected to rigorous purification procedures. Films (40–100 nm) of these polymers were deposited by spin coating (2000 rpm 40 s) from toluene solutions onto different substrates.

For conventional ellipsometry, fused silica (Spectrosil B) substrates were used. For interference enhancement ellipsometry we used substrates consisting of a 1-μm-thick silicon dioxide layer on top of a silicon wafer. In the case of aligned samples, the polymer film was deposited on top of a rubbed $\sim$30-nm-thick polyimide (PI) film, on top of the SiO_2/Si and fused silica substrates. The PFO and F8BT samples were then aligned in their nematic phase before rapid quenching back to room temperature. Further details of the alignment procedure can be found in the literature[27] (see also Sec. VI).

Ellipsometry data were collected using a reflection mode variable angle spectroscopic ellipsometer, GESP5 by SOPRA. Usually, five incidence angles (θ) were measured within a range ± 6 deg of the Brewster angle for each sample. The wavelength was scanned across the spectral range from 250 to 850 nm, with 3 nm steps. Further details will be given below.

III. THIN FILM ANISOTROPIES

When light propagates in a thin layer the electromagnetic (EM) boundary conditions for the TE and TM modes are

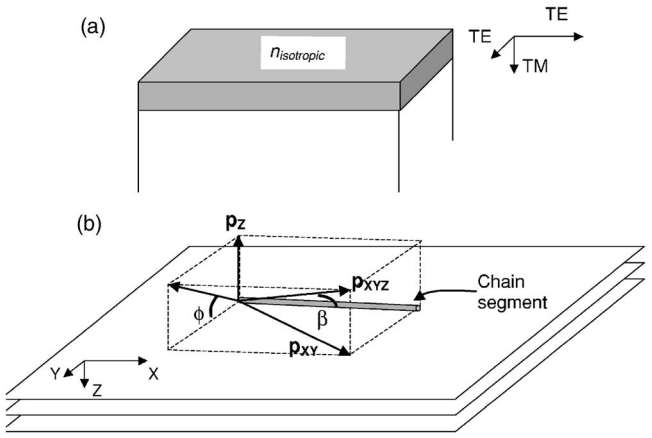

FIG. 2. (a) TE and TM directions for a thin film; (b) Definition of the angles for the upper limit model of the material anisotropy: All the chains are assumed to lie in planes parallel to the plane of the substrate.

different.[28] This is the basis of the theory of waveguides and a straightforward example of EM anisotropy; schematically shown in Fig. 2(a). The *X* and *Y* directions have equivalent EM boundary conditions which differ from those in the *Z* direction. Hence, in any thin film there is an in-plane/out-of-plane anisotropy independent of whether the material is itself isotropic or not. We shall call this the *EM anisotropy*. In addition, the material may itself be anisotropic, independent of the fact that it is in a thin film format. A polymer film that exhibits molecular orientation is one such example. This is the *material anisotropy*. The total anisotropy is then the combination of these two effects. A third situation might also arise: A material is isotropic in its bulk form but becomes intrinsically anisotropic as a thin film, as for instance found for semiconductor quantum wells.

A. EM anisotropy

In order to estimate the EM anisotropy for a typical polymer, we calculate the effective TE and TM refractive indices of an asymmetric planar slab[28] consisting of a 98-nm-thick PFO film (as core) sandwiched between air and fused silica cladding layers. This is, in fact, a typical sample structure for amplified spontaneous emission (ASE) experiments.[29] We employ the refractive indices of Spectrosil B ($n=1.462$), isotropic PFO (at the ASE wavelength: 466 nm, deduced for a 98-nm-thick film, $n=1.806$), and air ($n=1$); details of the calculation can be found in any standard book on integrated optics.[28] EM anisotropies of $\Delta n_{EM} \sim 0.06$ are found, which is the same order of magnitude as the Δn reported for several blue arylamine/fluorene copolymers (~ 0.05).[23] We also find good agreement between the predicted cutoff thicknesses (below which there are no bound propagation modes) and those observed in ASE experiments.[19,29].

Table II summarizes the EM anisotropy calculated for five polyfluorenes, assuming a film thickness of 100 nm, at the ASE wavelength. On the whole, however, these Δn values are smaller than the typical values reported in the literature ($\Delta n \sim 0.2$). This clearly implies that the EM anisotropy alone cannot account for typical Δn values.

B. Estimation of an upper limit for the material anisotropy

The intrinsic anisotropy of a polymer thin film is due to molecular order. Experimental evidence for such orientation in films of CPs comes not only from measurements of the optical anisotropy, but also from other experiments such as Raman depolarization ratio measurements[30,31] and x-ray diffraction.[32,33]

Each chain segment has an effective associated dipole that represents the first dipole-allowed highest occupied molecular orbital (HOMO) to lowest unoccupied molecular orbital (LUMO) optical transition and its vibronic substates. In general, the dipole will lie at an angle β with respect to the segment backbone.[34] The optical anisotropy in the transparency region is then fundamentally determined by the degree of orientation of, and the spatial averages for, this intrinsic dipole.

To get an estimate for the maximum value of this anisotropy, we consider the case of a film in which all the chains lie in planes parallel to the substrate; it is composed of layers of chains with chain segments performing random walks in each plane. One such segment in a plane is shown in Fig. 2(b). There are no segments oriented perpendicular to the substrate in this model. Consider also the case in which $\beta = 0$. This case gives the maximum possible anisotropy, because a field perpendicular to the plane will *not* couple to the dipoles. Therefore, as far as the effects of the optical gap (or first absorption band) are concerned, the anisotropy in the transparency region is maximum.

TABLE II. Difference between the effective refractive indices of the TE and TM modes for 100-nm-thick polymer core layers with refractive index $n_{polymer}$ (obtained from our own ellipsometric measurements), at the ASE wavelength. θ_{TE} and θ_{TM} are the critical angles for both modes, after Ref. 28.

		Electromagnetic anisotropy				
Material	λ (nm)	$n_{spectrosilB}$	$n_{polymer}$	θ_{TE} (rad)	θ_{TM} (rad)	Δn_{EM}
PFO	466	1.462	1.806	1.00	0.94	0.06
F6	466	1.462	1.870	1.00	0.91	0.10
F8DP	452	1.463	1.943	0.99	0.88	0.13
F8BT	576	1.455	1.904	0.94	0.87	0.08
Dow Red F	685	1.452	1.855	0.93	0.80	0.16

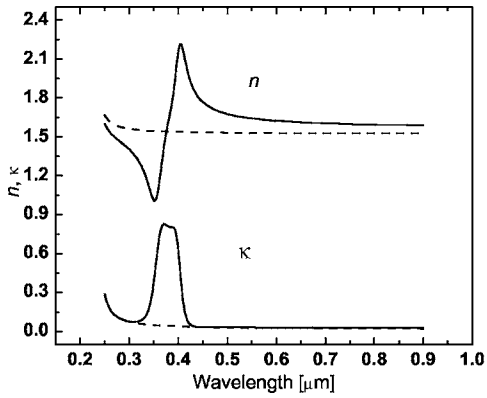

Material	ε_{iso}	$\varepsilon_{iso\ UV}$
F8BT	3.17	2.62
F6	2.90	2.60
PFO	2.52	2.33

FIG. 3. Isotropic complex refractive index (solid line) and UV contribution to the isotropic complex refractive index (dashed line) (shown here for PFO but representative of the general situation). The values of the dielectric function (at $\lambda=850$ nm) deduced for PFO, F6, and F8BT are summarized in the table.

Since the segments are randomly oriented, we need to average the polarizability in two dimensions (2D) and relate the oscillator strength of a single segment with that found in the isotropic phase. If α_p is the polarizability along the segment ($\beta=0$), segments which are randomly oriented in a plane yield an effective polarizability of $\alpha_p/2$ by averaging over all possible directions in the plane. The factor of two affects the oscillator strength seen by the incoming wave. In the isotropic case, the contribution in each direction is 1/3, so by performing a three-dimensional (3D) average one would recover the total oscillator strength. The effective oscillator strength for the film is then 3/2 of its value in the isotropic phase.

We now consider, for simplicity, the dielectric function for the isotropic case, ϵ_i, to be the sum of two terms: an UV contribution (the convolution of all UV transitions and hence mainly unpolarized) plus the absorption peak due to the HOMO-LUMO transition described above, which is polarized along the segment backbone ($\beta=0$). We produce the following model: from the dielectric function of the isotropic phase, we increase the oscillator strength of the first transition by 3/2 and leave all the other higher energy transition contributions the same. We recalculate the optical properties and assign this dielectric function to the *ordinary axis* of the film ($\epsilon_o=\epsilon_{in\text{-}plane}$). Then, we extinguish the HOMO-LUMO transition to obtain ϵ_{UV}. Since the dipoles are not coupled to the wave in the extraordinary direction, we can account for the out-of-plane dielectric function, $\epsilon_e=\epsilon_{out\text{-}of\text{-}plane}$ simply by taking ϵ_{UV}. From here we can deduce a maximum estimate for the birefringence below the lowest HOMO-LUMO transition of the polymer based on our extremely idealized description of the molecular order in the film. We have, accordingly,

$$\Delta\epsilon=\epsilon_o-\epsilon_e=\left[\tfrac{3}{2}(\textit{first-abs-band})+\epsilon_{UV}\right]-\epsilon_{UV}=\tfrac{3}{2}(\epsilon_i\text{-}\epsilon_{UV}). \tag{1}$$

We can take ϵ_i as the square of the refractive index deduced using isotropic fits, and calculate ϵ_{UV} simply by setting to zero the amplitude of the first HOMO-LUMO transition. An example of the refractive indices, n_i and n_{UV} deduced in this way for PFO is shown in Fig. 3.

The oscillator strength is directly proportional to $\epsilon(\omega)$, and not to the index of refraction which is $\propto\sqrt{\epsilon}$. The anisotropy in $\epsilon(\omega)$ ($\Delta\epsilon$) can be transformed into an anisotropy in n by means of

$$\Delta n\sim\sqrt{\frac{\epsilon_i+\epsilon_{UV}}{2}+\frac{\Delta\epsilon}{2}}-\sqrt{\frac{\epsilon_i+\epsilon_{UV}}{2}-\frac{\Delta\epsilon}{2}}. \tag{2}$$

From this extreme description, we obtain the following upper limits for the material anisotropy: $\Delta n_{PFO}\cong 0.09$; $\Delta n_{F6}\cong 0.14$; and $\Delta n_{F8BT}\cong 0.24$. (We have used the values at $\lambda=850$ nm in the table of Fig. 3.) We observe that for arylamine/fluorene copolymers, the values reported in the literature are considerably lower than these upper limit values ($\Delta n_{PFB}\sim 0.06$ and $\Delta n_{TFB}\sim 0.05$, from Ref. 23). This is consistent with their non-crystalline, non-liquid crystalline character and, hence, tendency to form isotropic glassy films. However, the anisotropy reported for F8BT (Ref. 22) (~ 0.3) exceeds the limit for perfect alignment (but see below). Note that our calculated values come from extremely idealized conditions in which $\beta=0$ (in Fig. 2) and there is a planar conformation for the segments. Neither of these conditions are remotely satisfied in real samples:We deduce $\beta=22$ deg for F8BT from Raman anisotropy and optical dichroism measurements on oriented films.[34] The fact that some of the reported values are close to our upper limits suggests that the anisotropies reported in the literature may sometimes be overestimated.

A more precise model needs to take into account the angle β and a specific distribution of chain directions out of the plane. Note that both effects decrease the anisotropy and, therefore, for an absolute upper limit estimate of Δn, Eqs. (1) and (2) may be used. When the dipole subtends an angle β with respect to the segment backbone direction, X, we need to recalculate the averages. If Φ is the angle formed by projecting β in the plane perpendicular to X with respect to the surface plane (see Fig. 2), we can average Φ between 0 and 2π. The anisotropy is in this case given by

$$\begin{aligned}\Delta\epsilon(\beta)&=\epsilon_o-\epsilon_e=\left[\frac{3}{2}\cos^2\beta-\frac{3}{4}\sin^2\beta\right](\epsilon_i-\epsilon_{UV})\\&=\Delta\epsilon(\beta=0)\left[\cos^2\beta-\frac{\sin^2\beta}{2}\right].\end{aligned} \tag{3}$$

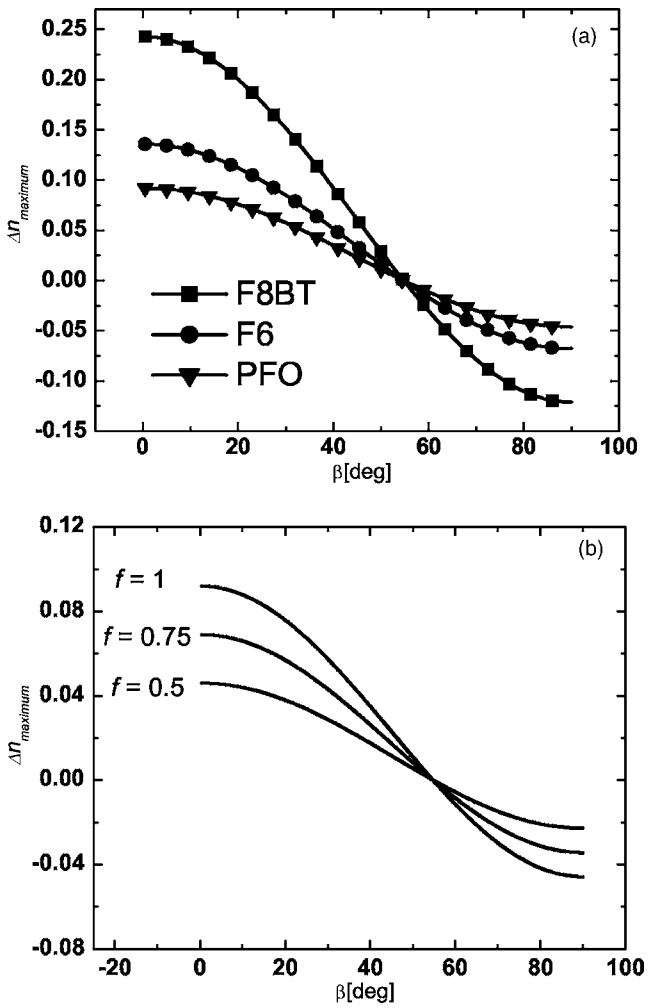

FIG. 4. (a) Maximum anisotropy, Δn, deduced for PFO, F6, and F8BT; (b) Maximum Δn derived for a distribution of PFO polymer chains consisting of f% lying parallel to the plane of the substrate and $(1-f)$% isotropically distributed. Both sets of data are plotted as a function of the angle β between the HOMO-LUMO transition dipole moment direction and the polymer chain segment projection axis. $\beta \sim 22$ and 26 deg for F8BT and PFO, respectively.

Figure 4(a) shows how the upper limit of the anisotropy, Δn, varies with β, for PFO (solid triangles), F6 (solid circles) and F8BT (solid squares). Equation (2) was used with $\Delta\epsilon$ given by Eq. (3). Typical values of $\beta \sim 20$ deg (see Ref. 34) would substantially decrease the anisotropy. It is interesting to note that for $\beta \cong 55$ deg, a perfect layering of molecules in planes parallel to the substrate would behave as an isotropic material.

A qualitative estimate for the distribution of molecular orientations on the other hand can be made by using an equivalent approach to Fraser's model,[35] where a fraction f of the total number of chains lie perfectly along one direction (parallel to the substrate) and the rest $(1-f)$ are isotropically distributed. This can be implemented within our model simply by changing the factor of 3 from the total oscillator strength of the isotropic dielectric function, to $3f$ in Eq. (3), i.e.,

$$\Delta\epsilon(\beta,f) = \epsilon_o - \epsilon_e = f\left[\frac{3}{2}\cos^2\beta - \frac{3}{4}\sin^2\beta\right](\epsilon_i - \epsilon_{UV})$$
$$= f\Delta\epsilon(\beta=0)\left[\cos^2\beta - \frac{\sin^2\beta}{2}\right]. \quad (4)$$

The result is shown in Fig. 4(b) for the case of PFO and three values of f, namely 1, 0.75, and 0.5. If we had only 50% of the PFO monomers perfectly oriented parallel to the substrate, then the maximum Δn_{PFO} would decrease to ~ 0.045.

It is important to mention that this approach is possible because we can separate the contribution of the lowest lying transition from the UV convolution of transitions. In this sense, having a parametric model for the dielectric function is an advantage.

There are two main approximations in this analysis. First, the UV contribution is unpolarized. This is not totally correct. The absorption spectra of aligned polyfluorene copolymers shows that whilst the difference between the absorption parallel (α_s) and perpendicular (α_p) to the chain decreases towards the UV,[27] it does not entirely vanish. This results, however, in a small correction below the gap, which is basically dominated by the lowest lying transition.

In the case of F8BT, we estimated a maximum anisotropy including the effect of the UV contribution to be $\Delta n(850\ \text{nm}) \sim 0.4$. This value was obtained by calculating ϵ_{UV} with the two main absorption peaks in the visible supressed (instead of only the lowest lying transition). This value compares better with the reported values at long wavelength (~ 0.3, from Ref. 22) but this is still for the extreme case with $\beta = 0$ deg and all segments lying in parallel planes. For PFO and F6, however, the higher energy contributions are not very polarized, making the previous predictions more reliable. This suggests that a knowledge of the dielectric function and its polarization over a large spectral range helps to estimate the maximum anisotropy more accurately.

The second approximation is that Δn in Eq. (2) is determined using an average dielectric function calculated from $(\epsilon_i + \epsilon_{UV})/2$. Since the isotropic fit retrieves mainly the refractive index in the plane of the substrate (see below), this is not, in fact, an approximation that underestimates the values of Δn and, hence, the upper limit is still valid. (Note that Δn increases as ϵ_i increases, and therefore, taking ϵ_o instead of ϵ_i would give even larger Δn values.)

IV. ROTATING POLARIZER REFLECTION ELLIPSOMETRY CONSIDERATIONS

A. Ellipsopmetry modeling issues

Unlike other optical techniques, modeling is an essential part of the information retrieval from ellipsometry. A single set of data can be interpreted sometimes by different models; it is an essential part of the data analysis process to judge the degree of accuracy and reliability of the model. One could argue that, even if ellipsometry is able to measure anisotropies in thin films, problems can still rise when trying to fit the ellipsometric data. Therefore, we discuss this issue fur-

TABLE III. Standard deviations, σ for the fitting of the ellipsometric angles calculated for an uniaxial thin film with an asymmetric absorption band.

Modeling of uniaxial films		
Model	No. of parameters	$\sigma 10^3$
Isotropic, 1 Lorentzian	6	2.332
Isotropic, 2 Lorentzians	9	1.659
Isotropic, 3 Lorentzians	12	1.563
Isotropic, 4 Lorentzians	15	1.509
Anisotropic, 1 Lorentzian	12	1.164
Anisotropic, 2 Lorentzians	18	0.308
Isotropic, 1 exciton	5	2.073
Isotropic, 2 excitons	9	1.480
Isotropic, 3 excitons	13	1.412
Anisotropic, 1 exciton	10	10^{-6}

ther before we turn to an analysis of the capabilities of the experimental technique.

We have performed a systematic study of the fitting process by first using model cases, and then the real data. We started by calculating the ellipsometric angles $(\cos\Delta, \tan\Psi)$ that a 100-nm-thick film with isotropic dielectric function deposited on a glass substrate would produce in reflection for five different incidence angles between 55 and 65 deg. We chose to generate the data using an asymmetric peak (excitonic) centred in the visible and with $\kappa_{max} \sim 1$, in order to simulate the real situation more closely. We then fitted the *computer generated data* using symmetric Lorentzian peaks, as done by many authors in the literature. We observed that the standard deviation of the fit decreases from 1.73×10^{-3} to 0.63×10^{-3} when using one and three Lorentzian peaks, respectively. This shows how in order to fit one asymmetric peak, a plethora of nonphysical peaks needs to be included. On the other hand, we fitted the isotropic data with an uniaxial model (consisting of one Lorentz peak for the ordinary plane, and another for the extraordinary direction). Surprisingly, the standard deviation for this unreal situation is 0.621×10^{-3}, even lower than using three peaks for the isotropic model. This gives the first warning that multiple parameter fits can be very misleading.

Subsequently, we calculated the ellipsometric angles $(\cos\Delta, \tan\Psi)$ for an uniaxial film on glass, with slightly asymmetric extinction coefficient and the typical values for CPs from the literature ($\Delta n \sim 0.2$ in the transparency region far from the lowest lying transition). We used the exciton model with one peak for each index to generate these data. We fitted the computer generated data using isotropic and anisotropic models for Lorentz and excitonic peaks. The results are summarized in Table III. We note that, consistent with our previous observations, the exciton model leads to smaller standard deviations when analyzing asymmetric absorptions. However, the main conclusion we would like to highlight by looking at the standard deviations is that anisotropic models fit considerably better the ellipsometric angles of an uniaxial layer than isotropic models do, at least, in ideal cases. This would suggest that, if an anisotropy of the order of 0.2 exists, ellipsometry should, then, be able to measure it. We note, further, that the software (WinElli by SOPRA) is self-consistent, as expected, and retrieves exactly the same optical constants when the model used to generate the data is used to fit the data, independent of the initial conditions ($\sigma \cong 0$).

However, when analyzing experimental data for CPs the results are somewhat different. By beginning with random (but physically possible) anisotropic optical constants, the iterative fitting process usually converges to unphysical results (such as negative absorptions). In all the cases reported in the literature, and due to the fact that the physical nature of the ordinary and extraordinary lowest lying transitions is the same, $\kappa_{in\text{-}plane}$ has the same dispersion as $\kappa_{out\text{-}of\text{-}plane}$. The oscillator strength is, however, higher for $\kappa_{in\text{-}plane}$ than for $\kappa_{out\text{-}of\text{-}plane}$ (and sometimes, very slightly redshifted). Therefore, it seems a good approach to set the initial conditions for both indices the same, and equal to that obtained using an isotropic fit. To start with, the excitonic amplitudes (which are proportional to the oscillator strength) are fitted. This process leads to a slight decrease in standard deviations ($\sim$5% better) for some cases (e.g., PFO and F8BT), but for other polymers, there is no improvement at all (such as in F6). The most delicate issue is that, even if some fits are better, the reliability of the results is not guaranteed. In fact, by modifying the initial conditions slightly, a different extraordinary index is obtained. This suggests that the fitting process is at the limit of confidence when including an anisotropic model. If we release the constraints (we allow the amplitudes and the energies to be freely fitted), this results in optical constants which are not physically possible (especially those of the extraordinary index). This is in agreement with Ramsdale *et al.* who found that fits of only reflection ellipsometry data produce very correlated parameters.[22] This situation can be improved by combining reflection and transmission ellipsometry, as they did in their study. The main message up to this point is that sensitivity problems might be playing a role in many reported values and that the real anisotropy in experimental situations must be smaller than $\sim$0.2 for PFO.

B. Ellipsometry measurement issues

Having tested the sensitivity of the fitting process against computer generated data, we focus now on the sensitivity of the experimental technique itself. Digman and co-workers found as early as 1971 that, in the limit of very thin films, reflection ellipsometry was not sensitive enough to measure the anisotropy of a uniaxial (Z in Fig. 2) film bounded by isotropic media.[36] This problem occurs only if the thickness of the film, d is much smaller than the wavelength of light, i.e., $d \ll \lambda$. The Digman result is, then, fully applicable for monolayer films in the visible range. For a typical conjugated polymer film used for characterization and device fabrication ($d \sim 50$–200 nm) and typical visible wavelengths, $\lambda \sim 500$ nm, the requirement is clearly not totally fulfilled ($d/\lambda \sim 0.4$–0.1). However, it already gives a hint that there may be some experimental issues for the sensitivity of specular ellipsometry when attempting to measure anisotropies of

thin films. In fact, comparing ellipsomenty with other experimental techniques (like Raman depolarization ratios),[30,31,37] one would conclude that ellipsometry tends to be less sensitive to variations in degrees of molecular orientation than other techniques.

One might argue that the different Raman depolarization ratios seen in drop cast and spin coated samples are a manifestation of different types of order on a much smaller length scale ($\sim 1\ \mu$m) than that probed by ellipsometry [a few millimeters (mm)] and, accordingly, samples look more isotropic for ellipsometry. This is, however, not consistent with other experimental observations.[17] Similarly, we found no need for the inclusion of anisotropy when fitting VASE experimental data for PFO samples where Raman measurements clearly show different degrees of molecular alignment (judged by differing depolarization ratios across mm distances).

To sum up, a combination of factors makes reflection ellipsometry of thin films deposited on glass substrates inadequate to measure uniaxial anisotropy. These factors include a high correlation of fitting parameters, poor reliability of the deduced anisotropic optical constants, the theoretical limitations of ellipsometry itself (in the thin film limit), and low experimental sensitivity to microscopic morphology changes.

V. INTERFERENCE ENHANCEMENT ELLIPSOMETRY

As discussed above, reflection ellipsometry with a rotating polarizer cannot retrieve the anisotropic optical constants of thin films accurately; a more sophisticated technique is required.

An anisotropic system can be totally characterized by 12 uncorrelated quantities at each energy. These are three real and three imaginary principal components of the dielectric tensor and their respective orientations (three Euler angles each). Theoretically, the analysis of general anisotropies by ellipsometry was formulated by Azzam and Bashara[38] and termed generalized ellipsometry (GE). GE can be implemented, for instance using two rotating compensators[39] or polarised modulators.[40] These techniques allow the determination of the 16 components of the Muller Matrix and, therefore, full characterization of the optical anisotropy.[41] Other techniques, such as the β-scan method (BSM) can also be used to solve the general anisotropic case.[42] The main inconvenience of these techniques is that they require a complicated (and different) setup (GE), experiment (BSM), and/or analysis of the data (GE and BSM).

Thin CP films, however, are expected to be uniaxial. Therefore, the number of unknowns is 4 at each energy: $\bar{n}_o = n_o + \kappa_o$ in the plane, and $\bar{n}_e = n_e + \kappa_e$ out of plane. We may take advantage of this high degree of symmetry to try to find a technique that enhances the experimental sensitivity to anisotropy.

Another (less appealing) possibility is to use multiple sample analysis,[43] where the ellipsometric angles for several films of the same material and different thicknesses are fitted at the same time. This approach has been already used for CPs.[21,25] However, the main assumption that the optical properties do not change with the layer thickness, is rarely true for CPs as the authors of Ref. 25 have themselves shown.[17] A further possibility is to combine reflection ellipsometry with either transmission spectroscopy[24,44,45] or transmission ellipsometry[22,23] and perform a global fitting process. These approaches have the disadvantage that two experiments need to be carried out instead of one, and that not all experimental ellipsometry setups allow transmission experiments. In any case, transmission experiments may not be the most suitable for measuring out-of-plane anisotropy since the changes in the transmitted beam due to the birefringence are not large due to the small film thickness ($d \sim 50-200$ nm).

In this section we use instead interference enhancement variable angle spectroscopic ellipsometry (IEVASE)[43] as a technique that can help to determine the optical anisotropy of thin CP films. We will use the case of a thin PFO film to study the sensitivity of the measurement for the characterization of out-of-plane birefringence.

A. Basic concepts

A typical sample for IEVASE measurement consists of the thin film deposited onto a silicon substrate that has a ~ 1 -μm-thick layer of SiO_2 on top, see Fig. 5(b). IEVASE relies on the fact that light is now reflected several times in the intermediate transparent SiO_2 layer. This layer has a thickness comparable to λ and, therefore, a spectral interference pattern is created in the reflection coefficients and in the ellipsometric angles. The periodicity of the fringes will depend upon the SiO_2 thickness and refractive index, but also on the boundary conditions, i.e., the optical constants of silicon and the polymer film, and the thickness of the latter. Since the optical constants of silicon and SiO_2 can be taken from the literature,[46] the thickness of the SiO_2 layer can be easily extracted from a direct inversion of the ellipsometric angles,[47] prior to spin coating the polymer.

The two main advantages of IEVASE with respect to transmission-reflection ellipsometry are that: (i) the same setup for reflection ellipsometry can be used, and (ii) due to the multiple reflections taking place, intrinsic effects of the polymer layer, such as anisotropy, can be enhanced. Due to the extra information provided by the interference fringes, the fitting parameters are more easily decorrelated compared to conventional ellipsometry. It is important to note that, due to the high absorption coefficient of conjugated polymers ($\alpha \sim 2 \times 10^5$ cm^{-1}), the multiple reflections within the polymer layer are rapidly attenuated across the polymer absorption spectral range. SiO_2 is, however, transparent in the visible range.

B. Anisotropic optical constants of spin coated PFO

We have employed the IEVASE technique to deduce the optical constants of spin coated PFO. Figure 6 shows the refractive index and extinction coefficient of PFO in-plane (solid line) and out-of-plane (dashed line), derived using three exciton peaks for each index. The film shows uniaxial anisotropy with the ordinary index parallel to the surface

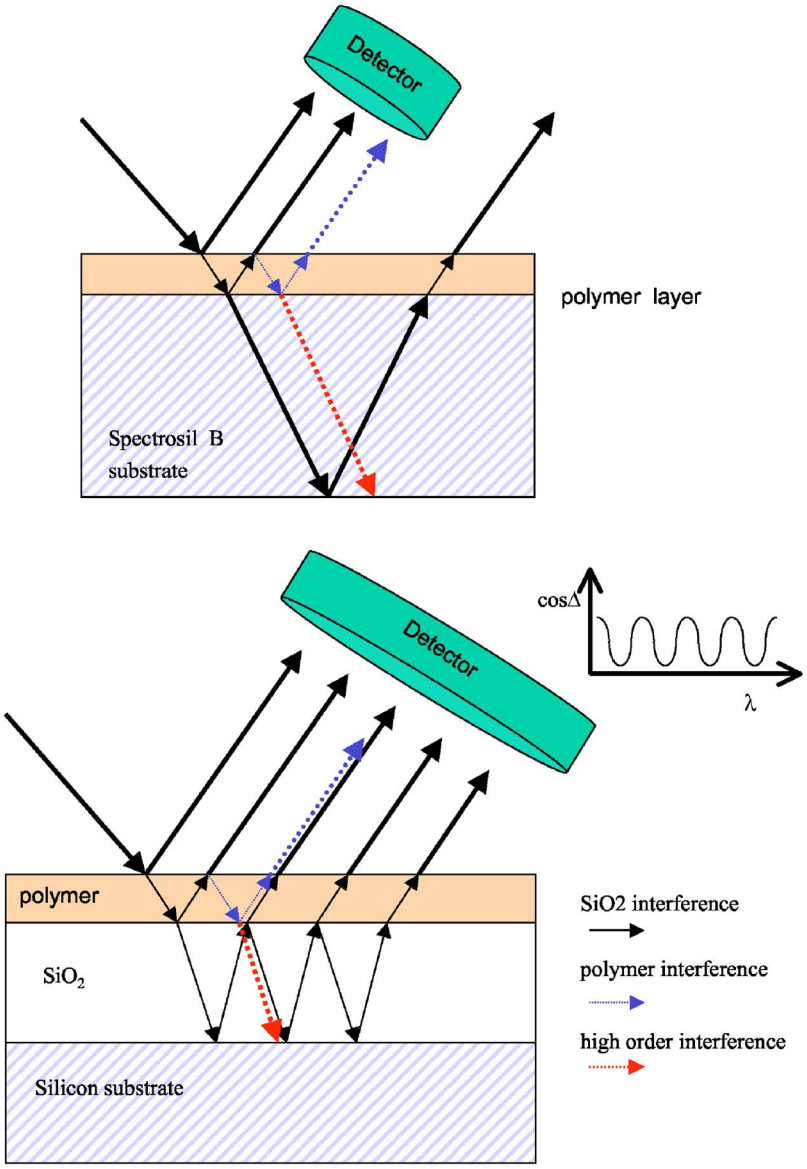

FIG. 5. (Color online) (a) Schematic of the reflection ellipsometry experiment, (b) schematic of Interference enhanced ellipsometry experiment. In the first case, the light collected by the detector is a combination of beams reflected from the polymer-air and polymer-substrate interfaces. In (b) the light bounces multiple times (due to the high reflectivity of Si) within the intermediate SiO_2 layer. The light collected by the detector has now been transmitted through the polymer layer many times, thus enhancing the sensitivity to material properties.

plane and the extraordinary index perpendicular to the substrate. This is in accordance with the reported anisotropies in spin coated conjugated polymers. The in-plane index presents higher oscillator strength (corresponding with preferential order of the polymer chains on the surface plane) than the out-of-plane index. The $\pi-\pi^*$ transition of the extraordinary index is slightly blueshifted, $\sim 10\pm 3$ nm. This has been attributed to a small reduction of conjugation length in the perpendicular direction.[22] The dichroic ratio, D (between the extinction coefficient maxima) is $D=\kappa_{ordinary}/\kappa_{extraordinary}=2.45$. The angular distribution, $d_{\pi\theta}$, defined as

$$d_{\pi\theta}=\frac{1}{(1+\kappa_{out\text{-}of\text{-}plane}^{\pi-\pi^*}/2\kappa_{in\text{-}plane}^{\pi-\pi^*})} \tag{5}$$

can be used as a measure of the degree of chain ordering.[12] $d_{\pi\theta}$ is equal to 2/3 for isotropic samples and tends to 1 with an increasing degree of anisotropy. For spin coated PFO, it has a value of $d_{\pi\theta}=0.83$, revealing a similar anisotropy to published values for other polymers [$d_{\pi\theta}=0.9$ for BCHA-PPV and $d_{\pi\theta}=0.84$ for MEH-PPV from Ref. 12, $d_{\pi\theta}=0.91$ for MEH-PPV from Ref. 18, $d_{\pi\theta}\sim 0.82$ for 5 poly(arylenephenylene)'s from Ref. 20].

The refractive index in the transparency region is higher in the ordinary direction than in the extraordinary direction. In particular, at the wavelength where amplified spontaneous emission occurs for this material, namely 466 nm,[29] the difference in refractive index is $\Delta n(466\text{ nm})=n_{in\text{-}plane}-n_{out\text{-}of\text{-}plane}\cong 1.84-1.70\cong 0.14$. The anisotropy rapidly decreases, as shown in Fig. 6 (left), as the wavelength moves away from the lowest lying transition. In particular, at 850 nm, $\Delta n=1.66-1.63=0.03$. This value is consistent with the upper limit value deduced for PFO at the same wavelength, $\Delta n_{max}(\beta=0)\sim 0.09$. If we take $\beta_{PFO}\sim 26.5°$ from Raman studies,[34] $\Delta n_{max}(\beta=26.5°)\cong 0.064$, which is in closer agreement. The difference between the upper limit and the measured value for Δn is accounted for by disorder in the segment orientations.

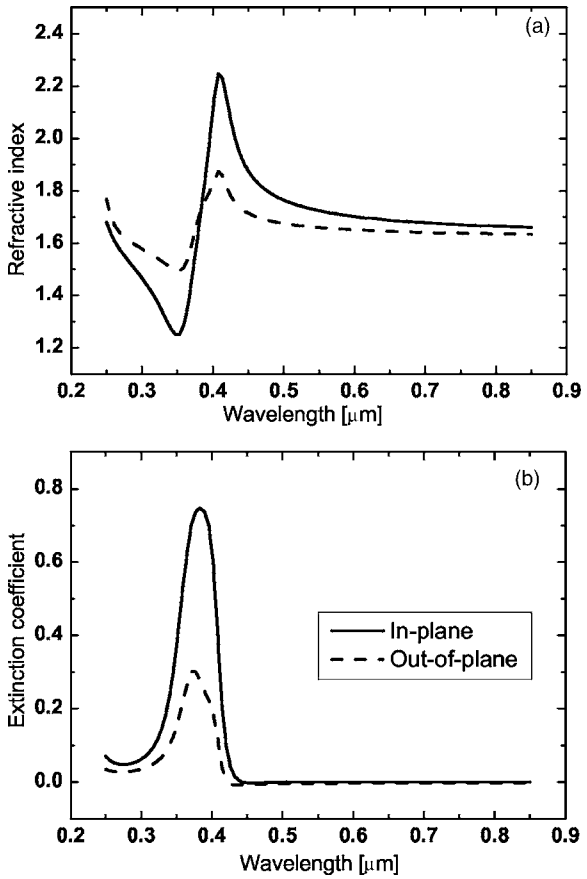

FIG. 6. In-plane (solid line) and out-of-plane (dashed line) dispersion of the complex refractive index of PFO. The anisotropic fit was for a 48-nm-thick PFO film on top of a 1020-nm-thick SiO_2 layer on top of a Si substrate.

The distribution factor f that would lead to this anisotropy can be deduced introducing Eq. (4) in [Eq. (2) =0.03], and this leads to a value of $f \sim 47\%$. If we assume a linear relationship between this model and the angular distribution of Ref. 12, the following expression is deduced $f = Ad_{\pi\theta} + B = 3d_{\pi\theta} - 2$ (the constants are chosen so isotropic and totally anisotropic limits are respected in both models). Using the value $d_{\pi\theta} = 0.83$, $f = 49\%$, in very good agreement with the value of f deduced from Eqs. (4) and (2).

We can, further, compare the deduced value of f using the two previous models with what one would obtain from the dichroic ratio, D, using the Fraser distribution[34,35]

$$f = \left(\frac{2}{3\cos^2\beta - 1}\right)\frac{(D-1)}{(D+2)}. \tag{6}$$

Introducing $D = 2.45$ and $\beta = 26.5°$, we obtain $f = 47\%$. This agreement between the three different determinations of f demonstrates a pleasing self-consistency and gives added confidence in the results.

C. Comparison between isotropic and uniaxial fits

When using IEVASE, isotropic models do not give a good fit. Figure 7(a) shows the wavelength dependence of the absolute value of the difference $\cos\Delta_{model} - \cos\Delta_{experiment}$, for the best fits of the ellipsometry data with isotropic (solid line) and uniaxial (dashed line) models. It is clear that an anisotropic model is needed to reproduce the interference fringes in the ellipsometric data and results in much lower standard deviations. The averages for N experimental points of the quantities

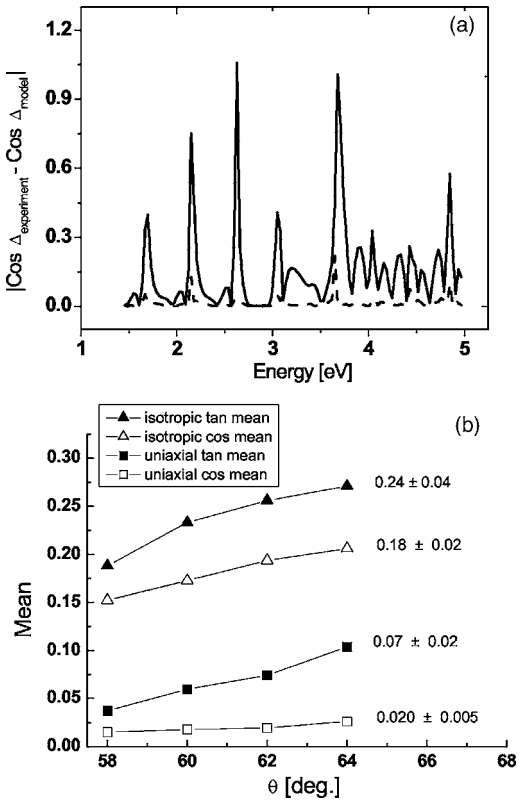

FIG. 7. (a) $|\cos\Delta_{isotropic} - \cos\Delta_{experimnet}|$ (solid line) and $|\cos\Delta_{uniaxial} - \cos\Delta_{experiment}|$ (dashed line) as a function of photon energy at $\theta = 54$ deg. (b) Mean values of $(\tan\Psi_{isotropic/uniaxial} - \tan\Psi_{experimental})$ and $(\cos\Delta_{isotropic/uniaxial} - \cos\Delta_{experimental})$ as a function of incidence angle, θ.

$$\langle \tan\Psi \rangle = \frac{\sum_i^N \|\tan\Psi_{model} - \tan\Psi_{experimental}\|}{N}, \tag{7}$$

$$\langle \cos\Delta \rangle = \frac{\sum_i^N \|\cos\Delta_{model} - \cos\Delta_{experimental}\|}{N}, \tag{8}$$

are 0.188 and 0.152 for the isotropic model, and 0.037 and 0.015 for the anisotropic model at an angle of incidence of 58 deg. These difference means are then one order of magnitude lower when uniaxiality is included.

Different incidence angles, θ, have different optical paths within the polymer layer, and, consequently the effect of the anisotropy on the ellipsometry data depends on θ. Light coming from wider angles with respect to the substrate normal will cover longer distances across the film, and will, as a result, undergo larger changes due to the anisotropy. Figure 7(b) shows $\langle \tan\Psi \rangle$ (solid symbols) and $\langle \cos\Delta \rangle$ (open sym-

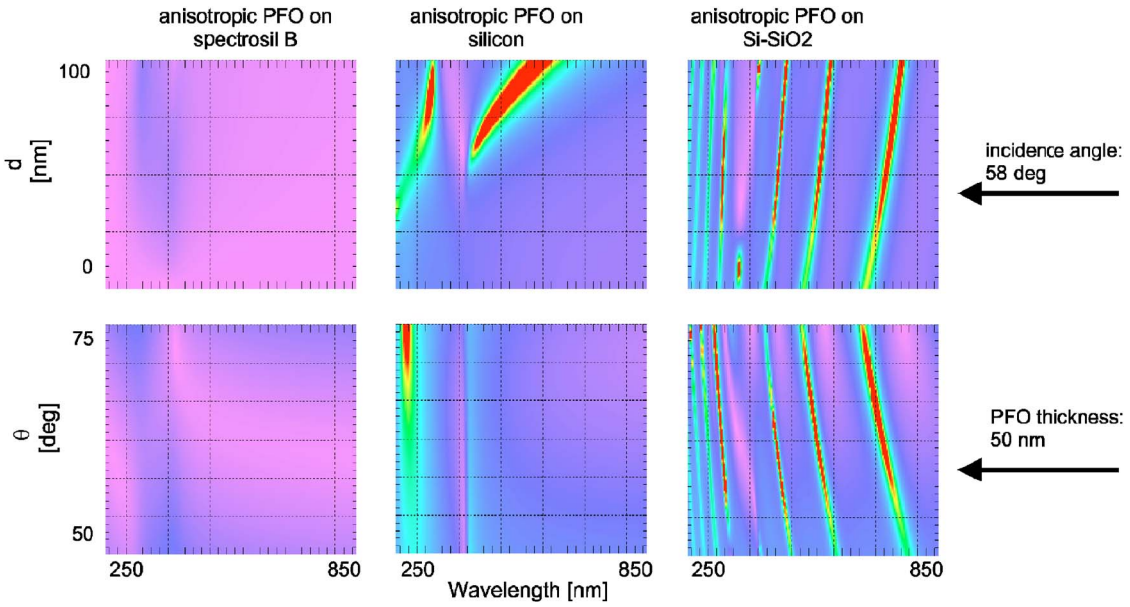

FIG. 8. (Color online) Comparison of tan Ψ data for PFO on Spectrosil B (left column), silicon (middle column), and silicon+SiO_2 (right column) substrates. The incidence angle (PFO film thickness) is fixed at 58 deg (50 nm) in the first (second) row. See text for more details.

bols) for four different incidence angles from 58 to 64 deg. The isotropic fit (triangles) gives higher standard deviations than the uniaxial fit (squares). In addition, as the incidence angle increases, the standard deviation of the isotropic fit increases, giving further confidence in the need for anisotropy. $\langle \cos \Delta \rangle$ vs θ is flat for the uniaxial model. The anisotropic $\langle \tan \Psi \rangle$ increases with increasing θ, less strongly in absolute value than when using isotropic models. When considering relative values (with respect to the initial value of $\langle \tan \Psi \rangle$), the increase is, however, larger for the anisotropic than the isotropic fits.

It is important to note that *the refractive index deduced using an isotropic model does not correspond to an average refractive index*, i.e., $n_{isotropic\text{-}model} \neq n_{isotropic} = \frac{2}{3} n_{ordinary} + \frac{1}{3} n_{extraordinary}$. Instead, it corresponds to the ordinary index deduced with the uniaxial model.[48] This is a key point. When analyzing reflection ellipsometry data of an uniaxial thin film with an isotropic model, the deduced optical constants correspond to the in-plane optical constants $n_{isotropic\text{-}model} \cong n_{ordinary}$. This is consistent with the good match between normal incidence spectrophotometry and VASE found in most cases, and it has also been observed when fitting computer generated anisotropic data with isotropic models as described in Sec. VI A. As such, it is another manifestation of the insensitivity of reflection ellipsometry to out-of-plane anisotropies unless multiple reflections are used.

D. Comparison between substrates

We will briefly show how IEVASE is generally more sensitive than conventional VASE when dealing with uniaxial thin films. To this end, we have modeled the ellipsometric angles produced by the following five systems: a 100-nm-thick PFO film on a Spectrosil B substrate, and a 100-nm-thick PFO film on a 1 μm SiO_2 layer on a Si substrate, for both, isotropic and anisotropic polymer layers. We have also considered a 100-nm-thick anisotropic PFO film on a silicon substrate. The first substrate corresponds to a conventional VASE setup within the field of organic semiconductors, while the second corresponds to IEVASE. The bare silicon substrate was also modelled for completeness. We can, first, compare the spectroscopic average of $|\tan \Psi_{isotropic} - \tan \Psi_{uniaxial}|$ for both Spectrosil B and SiO_2/Si substrates as a way to quantify the sensitivity of the two techniques to uniaxial anisotropy. In general, a technique will be more sensitive when the difference between isotropic and anisotropic is larger. The calculated values are 0.315 and 0.057 for IEVASE and VASE, respectively. This shows the importance of the substrate in enhancing the sensitivity of the measurement to the anisotropic nature of the film.

Figure 8 shows the modelled mappings of tan Ψ (color scale online) as a function of wavelength, film thickness and incidence angle. In the first row of the graphs, the incidence angle was fixed at 58 deg and the thickness of the anisotropic PFO was varied from 0 to 100 nm. The second row has fixed thickness $d=50$ nm, and shows the variation with angle for $50 \text{ deg} < \theta < 75$ deg. The online color scale refers to (violet) $0 < \tan \Psi < 3$ (red). The first and second columns correspond to VASE with Spectrosil B and silicon substrates, respectively. The last column shows the results for IEVASE (SiO_2/Si substrate).

A number of comments can be made about Fig. 8. First, the range of values of tan Ψ is around six times larger in IEVASE than in conventional VASE with Spectrosil B substrates. Compared to VASE with silicon substrates, IEVASE is around twice as large (note that if a wider color range had been chosen, the results for Spectrosil B would have shown no appreciable contrast). In addition, changes in the ellipsometric angles with wavelength are more abrupt and of larger magnitude in the case of IEVASE. This is, by itself, a proof of the higher sensitivity of IEVASE. Second, the position of

the maxima of the interference fringes is strongly dependent on both polymer thickness and incidence angle. This is an extra piece of information that helps to decorrelate the fitting parameters. IEVASE is, therefore, very sensitive to thickness variations, which would make this technique very promising not just for anisotropic polymer thin films, but also for films in the monolayer regime. The large variations of $\tan\Psi$ with incidence angle prove that IEVASE is very sensitive also to in-plane/out-of-plane anisotropies. Finally, the spectroscopic variation of the ellipsometric angles is also much stronger when the SiO_2/Si substrate is employed. Therefore, the dispersion of the optical constants can be accurately determined (if a good fit is achieved) by IEVASE.

VI. IN-PLANE ANISOTROPIES

Finally, we study a different type of anisotropy in CP thin films, namely: in-plane anisotropy. Since the demonstration of the first conjugated polymer light emitting diode in 1989,[49] there has been an increasing interest in organic semiconductors for optoelectronic applications. One particular field of research is their utilization for polarized light emission. Such devices would be potentially advantageous for liquid crystal displays as replacements for the backlight plus polarizer combination currently used. If one could align all the polymer chains in a single direction and provided the transition dipole aligns with the polymer chain axis, then, the emission would be perfectly polarized. In addition, the alignment process can increase the transport mobilities in transistor configurations[50] and reduce the amplified spontaneous emission threshold energies.[51] High degrees of molecular orientation have been achieved for several polyfluorenes.[27,52–54] Note, however, that the existence of a small but finite angle between the polymer chain and the dipole (see Fig. 2 and Sec. III B) makes a fully polarized device impossible.

CPs can be aligned by the application of a uniaxial stress, rubbing, or shear. One of the most promising ways is to use thermotropic liquid crystalline CPs; they can be aligned by deposition onto a rubbed layer and subsequent heating into the liquid crystalline phase. In this section, we characterize the optical constants of polymer films aligned by this procedure. We use interference enhancement VASE (described in the previous section) to resolve the anisotropic optical constants of PFO and F8BT. The interference pattern shown in the ellipsometric angles does not, in this case, enhance the sensitivity to anisotropy. It helps, however, to decorrelate the parameters of the multilayer structure. Note that for spin coated films the ordinary index lies parallel to the plane of the substrate and the extraordinary in the perpendicular direction ($n_{ordinary}=n_{in\text{-}plane}>n_{extraordinary}=n_{out\text{-}of\text{-}plane}$). For oriented films (see, e.g. Refs. 55–57), however, the extraordinary index lies along the chain direction (within the plane of the substrate), and the ordinary in the plane perpendicular to the chain direction (now $n_{extraordinary}=n_{chain\text{-}direction}>n_{ordinary}=n_{perpendicular\text{-}to\text{-}chain\text{-}direction}$).

A. Aligned polymers

As experimental examples, we have studied oriented polymer films (PFO and F8BT) of about 100 nm thickness

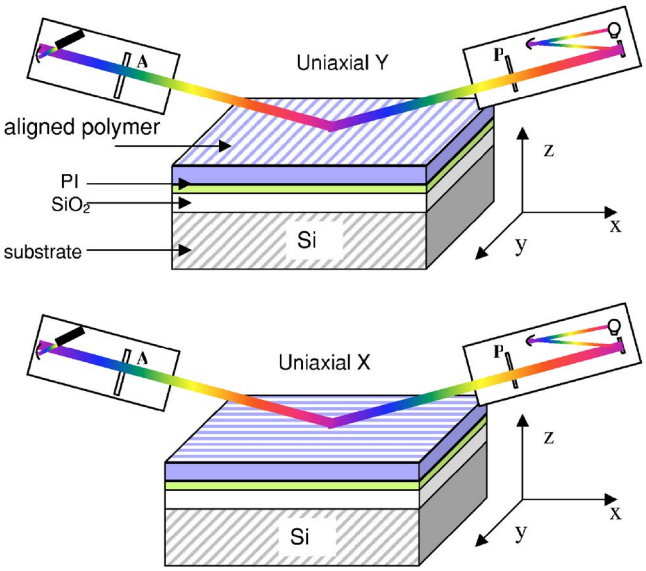

FIG. 9. (Color online) Experimental procedure to deduce the optical constants of aligned conjugated polymers. Two VASE measurements were taken for the Si/SiO_2/PI/polymer system, with the incidence plane lying parallel (or perpendicular) to the rubbing direction. The two sets of data were then analyzed together. P stands for polarizer and A for analyzer.

deposited on rubbed PI layers (40 nm thick), on top of SiO_2 intermediate layers on top of Si substrates. The SiO_2 layer was measured to be 1020 nm±2 nm in thickness prior to CP film deposition (we used the published refractive index values for Si and SiO_2 from Refs. 46 and 58). The PI alignment layer was spin coated and thermally treated following the usual procedure.[27,52] VASE was employed to characterize the dielectric function of PI. The PI layer was rubbed as an alignment layer and the optical constants were checked again. A negligible degree of anisotropy was found: The rubbing process causes a surface modification rather than producing a bulk alignment of the PI chains. This is consistent with previous results.[26] The CP layer was spin coated onto the rubbed PI, heated at 20°/min to a initial temperature (200° for PFO and 265° for F8BT), slowly cooled to a final temperature (170° for PFO and 235° for F8BT), and then rapidly quenched to room temperature. The result is a glassy polymer film with the polymer chains oriented in the rubbing direction (as confirmed by measuring polarized PL spectra).

Two IEVASE measurements were carried out with the incoming beam oriented to have its *E*-field direction either parallel or perpendicular to the rubbing direction, as shown in Fig. 9. The ellipsometry data were recorded at four different incidence angles around the Brewster angle of each sample, across a wavelength range from 250 to 850 nm (in steps of 2 nm).

When dealing with in-plane anisotropies, at least two different refractive indices should be considered. The extraordinary (ordinary) index will correspond to the direction parallel (perpendicular) to the rubbing direction.[55–57] It can be argued that aligned polymers may have biaxial behaviour as a combined result of the typical intrinsic material anisotropy (previous section) and the orienting process, but the differ-

ence between the refractive indices perpendicular to the substrate (Z in Fig. 9) and perpendicular to the rubbing direction and parallel to the surface [X in Fig. 9(a) and Y in Fig. 9(b)] is smaller than the experimental error. Therefore, in all the cases studied here, uniaxial models with the optical axis parallel to the rubbing direction have been employed to fit the ellipsometry data. This does not mean that the out-of-plane anisotropy has ceased to exist, but rather that its inclusion (via a biaxial model) requires a sensitivity which goes beyond even IEVASE.

Two exciton peaks have been included for each of the indices of PFO (ordinary and extraordinary), while 4 were used for F8BT. The fitting process consists of deducing the anisotropic optical constants of the oriented polymer for a set of values of the thickness of PI around those obtained before rubbing. This accounts for the possibility that during rubbing the thickness of the PI layer may decrease. In addition, the PI-polymer interface can be relatively rough, and this accounts for a possible finite interface thickness between the PI and the CP. The fitting involves about 20 different PI thicknesses and polymer optical constants divided in two sets. Uniaxial Y (uniaxial X) was employed when the fit was done over the data recorded with the experimental setup of Fig. 9(a) [Fig. 9(b)]. The PI thickness that leads to the smallest standard deviation is taken as the most likely value. The estimated errors are generally smaller than 1%. The error values of the refractive index and extinction coefficient are, here, referred to as δn and $\delta\kappa$, respectively. For PFO, $\delta n_{extraordinary} < 0.02$, $\delta n_{ordinary} < 0.15$, $\delta\kappa_{extraordinary} < 0.05$ and $\delta\kappa_{ordinary} < 0.12$; and for F8BT, $\delta n_{extraordinary} < 0.02$, $\delta n_{ordinary} < 0.03$, $\delta\kappa_{extraordinary} < 0.2$ and $\delta\kappa_{ordinary} < 0.03$.

B. Aligned PFO

Figure 10(a) shows the resulting extraordinary and ordinary refractive indices of oriented PFO with solid and dashed lines, respectively. Of particular interest for organic lasers is the birefringence at the amplified spontaneous emission wavelength, which in this case is $\Delta n(466\ \text{nm}) = n_o - n_e = 1.62 - 2.24 = -0.62 \pm 0.07$. At this particular wavelength, the refractive index of PI is smaller than the extraordinary refractive index of PFO, but higher than the ordinary index. This will have an important effect on the waveguiding conditions and on the polarisation of the ASE in planar wave guide structures.[59] Virgili *et al.* found $|\Delta n|$ of an aligned PFO layer embedded in a cavity structure to be ~ 0.36 for $\lambda \sim 480$ nm.[60] This value is considerably smaller than found in the present study. However, the photoluminescence (PL) dichroic ratio they found was considerably smaller than the absorption dichroic ratio deduced from Fig. 10 showing a different degree of molecular alignment in their samples. The degree of alignment is (at the experimental level) very sample dependent, and hence, the anisotropic optical constants also vary from sample to sample. Other samples studied in microcavities subsequent to Ref. [60] have shown $|\Delta n| \leqslant 0.65$, in better agreement with the results here.

The extraordinary and ordinary extinction coefficients of PFO are shown in Fig. 10(b) (the same labels apply). The main absorption peak is centered at 390 nm. The oscillator

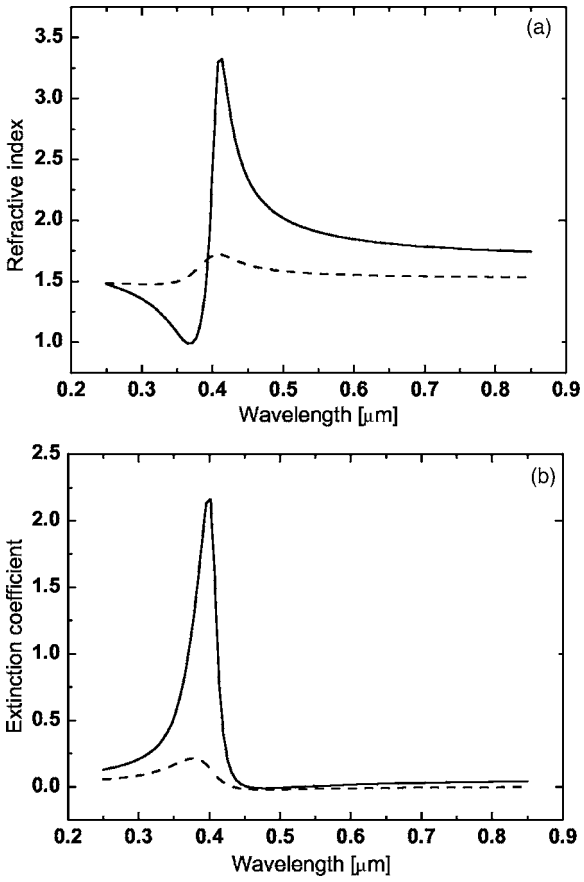

FIG. 10. Refractive index (a) and extinction coefficient (b) data parallel to the chain direction (solid line) and in the plane perpendicular to the chain direction (dashed line) for an oriented PFO film.

strength of the extraordinary peak is higher than that of the ordinary peak [$\kappa_e(\lambda_{max}) = 2.21 \pm 0.15$ and $\kappa_o(\lambda_{max}) = 0.21 \pm 0.15$], with the dichroic ratio, $D \cong 10$. Similar degrees of alignment have been reported before.[27] Note that even if the chains are perfectly aligned, the anisotropy would be finite due to the finite transition dipole moment angle $\beta \sim 26$ deg relative to the chain axis for PFO and ~ 22 deg for F8BT.[34] The absorption maximum for the ordinary index is slightly blueshifted (to 380 nm) compared to that of the extraordinary peak (at 402 nm). This may suggest that the chains oriented in the rubbing direction have a longer effective conjugation length.

Compared to spin coated films, oriented films have larger anisotropies Δn. The maximum of the extinction coefficient along the chain direction is 2.21, which is much larger than the in-plane κ (smaller than ~ 0.8). This is in agreement with Lyons and Monkman[26] who found that the difference between ordinary and extraordinary absorption coefficients is nearly twice as high for aligned poly(9,9-diethylhexyl fluorene) [PF 2/6] films than for spin coated films. The reason for this is that a large fraction of the chains now lie in one direction (instead of lying randomly distributed on a plane). Using similar arguments as before, we may deduce the upper limit of the anisotropy for oriented films. If we consider all the chains to be parallel and $\beta = 0$ the total oscillator strength of the lowest lying transition is distributed in the extraordinary direction and therefore

$$\Delta\epsilon = \epsilon_e - \epsilon_o = 3(\epsilon_i - \epsilon_{UV}). \quad (9)$$

Note that we do not include the 1/2 found in Eq. (1) from averaging in the plane. The upper limit for the anisotropy here is twice as large as in spin coated films (in terms of ϵ). By introducing Eq. (9) in Eq. (2), using the values for ϵ_i and ϵ_{UV} given in Sec. III B, the upper limit for the anisotropy of oriented films at $\lambda \sim 850$ nm is ~ 0.50, which is larger than the measured value [$\Delta n(850) \sim 0.21$]. We note that, for this calculation, we have used the isotropic refractive index of glassy PFO rather than the spin coated one. The values considered were $\epsilon_i = 2.641$ and $\epsilon_{UV} = 2.129$. If now we consider $\beta \neq 0$, and a Fraser like distribution we obtain

$$\Delta\epsilon = \epsilon_e - \epsilon_o = 3f(\epsilon_i - \epsilon_{UV})\left(\cos^2\beta - \frac{\sin^2\beta}{2}\right). \quad (10)$$

With $\beta = 26.5°$, f is $\sim 60\%$, i.e., 60% of the chains are ordered in the direction of the optical axis. This value is smaller than those reported by Liem *et al.*,[34] namely of order 75%. In fact, deducing f from the dichroic ratio [Eq. (6)], suggests that the sample should be 100% oriented. This probably comes from the large error in D deduced using this method. Using classical error propagation we have

$$\delta D = D\left(\frac{\delta\kappa_e}{\kappa_e} + \frac{\delta\kappa_o}{\kappa_o}\right) = 10\left(\frac{0.05}{2.21} + \frac{0.12}{0.21}\right) \cong 6.0. \quad (11)$$

The large relative error obtained for κ_o, makes the value of D very uncertain, i.e., $D = 10 \pm 6.0$. One could calculate the dichroic ratio that a distribution of molecules described by $f = 60\%$ would produce using Fraser's equation [Eq. (6)]. This value would be $D \sim 4$, which still is within the error. This example shows that, although IEVASE is generally more sensitive than conventional reflection ellipsometry, it, nevertheless, has certain limitations when dealing with complex systems such as multilayer structures or anisotropic samples.

C. Aligned F8BT

Figure 11(a) shows the extraordinary and ordinary refractive indices of oriented F8BT (solid and dashed lines, respectively) deduced from IEVASE. As for PFO, the extraordinary index is higher than the ordinary index. The birefringence at the ASE wavelength (576 nm) is in this case $\Delta n(576\text{ nm}) = n_o - n_e = 1.59 - 2.10 = -0.51 \pm 0.06$, i.e., smaller than for oriented PFO.

The extraordinary and ordinary extinction coefficients of F8BT are shown in Fig. 11(b). There are two main peaks in the absorption spectra of F8BT, which are centered at 310 and 455 nm, respectively. The latter corresponds to the promotion of an electron from the HOMO to a LUMO that is localized on the benzothiadiazole moiety.[61] The dichroic ratio is $D = 2.8$ for the more energetic peak and 10.8 for the peak at ~ 455 nm. This polarization dependence has already been observed in F8BT[22,27] and suggests that the transition dipole of the peak at ~ 310 nm subtends a greater angle (β) with respect to the chain axis than that of the lower energy peak. High energy transitions which are polarised off the chain axis have also been experimentally and theoretically demonstrated for aligned PPV by Comoretto and co-workers.[57]

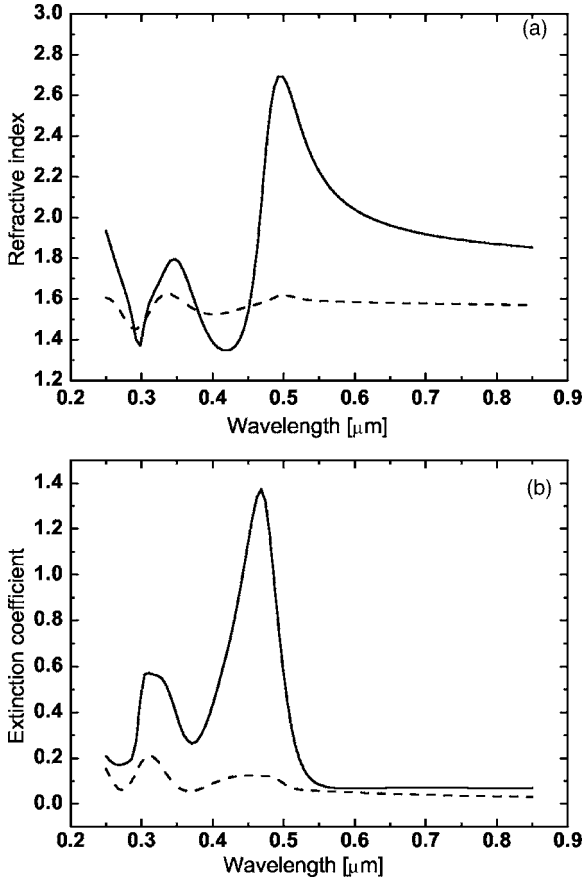

FIG. 11. Refractive index (a) and extinction coefficient (b) data parallel to the chain direction (solid line) and in the plane perpendicular to it (dashed line) for an oriented F8BT film.

In addition, there is a blueshift of 15 ± 5 nm from the extraordinary to the ordinary extinction coefficients for the peak centred at 455 nm suggesting a decrease in conjugation length. However, the second peak (310 nm) does not show any spectral shift. This can be explained if the excited state that leads to the peak at 310 nm is strongly localized and, hence, less anisotropic in nature.

VII. CONCLUSIONS

Different optical anisotropies in CP thin films were comprehensively analyzed with the aim of critically probing whether the large out-of-plane optical anisotropies reported in the literature are real, and investigating the limitations of reflection ellipsometry to determine such anisotropies. Two kinds of anisotropies were described: electromagnetic and material specific. The electromagnetic anisotropy arises from different boundary conditions for electromagnetic waves with **E** vectors vibrating parallel and perpendicular to the surface. The intrinsic anisotropy is due to preferential molecular ordering in the film. A model for the upper limit of the intrinsic anisotropy in the transparency spectral region was derived. Δn_{max} at $\lambda = 850$ nm was found to be 0.09, 0.14,

and 0.4 for PFO, F6, and F8BT, respectively. These upper limit values will be reduced in real samples when the angle β between the dipole moment and the chain segment director is taken into account, and the distribution of chain directions is appropriately averaged. In the case of spin coated PFO films, 47% of dipoles are estimated to lie parallel to the substrate plane. The upper limit value of F8BT is larger than the published anisotropy. However, a large number of values reported for films made of similar materials are comparable or go beyond this highly idealized limit. We found that a variety of reasons limit the sensitivity of ellipsometry for measuring in-plane/out-of-plane birefringence in thin films. These include a high correlation among fitting parameters when anisotropy is included in the model, theoretical limitations of ellipsometry itself in the thin film limit and low experimental sensitivity to microscopic morphology changes.

We have, therefore, proposed IEVASE as a possible technique to retrieve the optical anisotropy of CP thin films. This technique uses the interference pattern created by an intermediate layer to enhance the effects of an in-plane/out-of-plane anisotropy in the ellipsometric data. The in-plane and out-of-plane optical constants of spin coated PFO were, then, deduced using IEVASE. The results were consistent with the upper limit model and indicate a moderate degree of molecular ordering for this polyfluorene. Δn was found to be equal to 0.14 and 0.03 at $\lambda = 466$ and 850 nm, respectively. Additionally, we showed that the optical constants deduced with isotropic models correspond mostly to the in-plane contribution, and not to an average. This is, actually, a property of reflection ellipsometry which has been used for many years to measure weak optical anisotropies in uniaxially stressed semiconductors: reflection ellipsometry measures an effective index of refraction along a direction defined by the projection of the incident optical plane and the surface of the sample.[62] Thus, when applying reflection ellipsometry to spin coated films, this technique is mainly sensitive to the ordinary index, which is different from the isotropic average.

Finally, the anisotropic refractive index of oriented (in-plane) polymers was studied using IEVASE. As expected, the refractive index along the chain direction was found to be higher than that in the plane perpendicular to it. Again, as expected, higher degrees of anisotropy were deduced for aligned films of both PFO and F8BT compared to spin coated film samples.

ACKNOWLEDGMENTS

The authors thank the UK Engineering and Physical Sciences Research Council (EPSRC) for financial support via the Ultrafast Photonics Collaboration (GR/R55078). We also thank The Dow Chemical Company for providing the PFO and F8BT polymers that we have studied. PGE acknowledges support from an EPSRC grant (GR/T06124). MCQ acknowledges the hospitality of the McDiarmid Institute for Advanced Materials and Nanotechnology in New Zealand where part of this work was carried out.

*Electronic address: m.campoy@imperial.ac.uk
†Electronic address: pablo.etchegoin@vuw.ac.nz
‡Electronic address: d.bradley@imperial.ac.uk

[1] M. Campoy-Quiles, G. Heliotis, R. Xia, M. Ariu, M. Pintani, P. Etchegoin, and D. D. C. Bradley, Adv. Funct. Mater. **14**, 925 (2005).
[2] E. Hecht and A. Zajac, *Optics* (Addison-Wesley, New York, 1974).
[3] A. Sassella, T. Wagner, C. Herzinger, G. Su, Y. He, and C. Chen, Thin Solid Films **455–456**, 576 (2004).
[4] M. Friedrich, G. Gavrila, C. Himcinschi, T. U. Kampen, A. Y. Kobitski, H. Mendez, G. Salvan, I. Cerrillo, J. Mendez, N. Nicoara, J. Phys.: Condens. Matter **15**, S2699 (2003).
[5] J. N. Hilfiker, B. Johs, C. Herzinger, J. F. Elman, E. Montbach, D. Bryant, and P. J. Bos, Thin Solid Films **455–456**, 591 (2004).
[6] J. N. Hilfiker, T. Wagner, A. Marino, G. Delgais, and G. Abbate, Thin Solid Films **455–456**, 596 (2004).
[7] I. A. Badmaeva, L. A. Nenasheva, V. G. Polovinkin, S. M. Repinsky, and L. L. Sveshnikova, Thin Solid Films **455–456**, 557 (2004).
[8] G. Y. Guo, K. C. Chu, D. S. Wang, and C. G. Duan, Phys. Rev. B **69**, 205416 (2004).
[9] J. Tanaka and M. Tanaka, *Handbook of Conducting Polymers* (T. A. Skotheim, 1986), Vol. 2.
[10] H. Arwin, J. Martensson, and R. Jansson, Appl. Opt. **31**, 6707 (1992).
[11] H. Arwin and R. Jansson, Electrochim. Acta **39**, 211 (1993).
[12] D. McBranch, I. H. Campbell, D. L. Smith, and J. P. Ferraris, Appl. Phys. Lett. **66**, 1175 (1995).
[13] J. W. M. Prest and D. J. Luca, J. Appl. Phys. **50**, 6067 (1979).
[14] J. W. M. Prest and D. J. Luca, J. Appl. Phys. **51**, 5170 (1980).
[15] A. Boudrioua, P. A. Hobson, B. Matterson, I. D. W. Samuel, and W. L. Barnes, Synth. Met. **111–112**, 545 (2000).
[16] K. Koynov, A. Bahtiar, T. Ahn, C. Bubeck and H. Hörhold, Appl. Phys. Lett. **84**, 3792 (2004).
[17] V. Zhokhavets, G. Gobsch, H. Hoppe, and N. S. Sariciftci, Thin Solid Films **451–452**, 69 (2004).
[18] M. Tammer and A. P. Monkman, Adv. Mater. (Weinheim, Ger.) **14**, 210 (2002).
[19] E. K. Miller, M. D. McGehee, M. Diaz-Garcia, V. Srikant, and A. J. Heeger, Synth. Met. **102**, 1091 (1999).
[20] M. Losurdo, M. M. Ciangregorio, P. Capezzuto, G. Bruno, F. Babudri, D. Colangiuli, G. M. Farinola, and F. Naso, Macromolecules **36**, 4492 (2003).
[21] J. Sturm, S. Tasch, A. Niko, G. Leising, E. Toussaere, J. Zyss, T. C. Kowalczyk, K. D. Singer, U. Scherf, and J. Huber, Thin Solid Films **298**, 138 (1997).
[22] C. M. Ramsdale and N. C. Greenham, Adv. Mater. (Weinheim, Ger.) **14**, 212 (2002).
[23] C. M. Ramsdale and N. C. Greenham, J. Phys. D **36**, L29 (2003).
[24] L. A. A. Pettersson, F. Carlsson, O. Inganäs, and H. Arwin, Thin Solid Films **313–314**, 356 (1998).
[25] V. Zhokhavets, R. Goldhahn, G. Gobsch, and W. Schliefke, Synth. Met. **10291**, 1 (2003).

[26] B. P. Lyons and A. Monkman, J. Appl. Phys. **96**, 4735 (2004).
[27] K. S. Whitehead, M. Grell, D. D. C. Bradley, M. Jandke, and P. Strohriegl, Appl. Phys. Lett. **76**, 2946 (2000).
[28] T. Tamir, *Integrated Optics*, 2nd ed. (Springer-Verlag, Berlin, 1979).
[29] G. Heliotis, D. D. C. Bradley, G. A. Turnbull, and I. D. W. Samuel, Appl. Phys. Lett. **81**, 415 (2002).
[30] H. Liem, P. Etchegoin, K. S. Whitehead, and D. D. C. Bradley, J. Appl. Phys. **92**, 1154 (2002).
[31] H. Liem, P. Etchegoin, and D. D. C. Bradley, Phys. Rev. B **64**, 144209 (2001).
[32] T. Erb, S. Raleva, V. Zhokhavets, G. Gobsch, B. Stühn, M. Spode, and O. Ambacher, Thin Solid Films **450**, 97 (2004).
[33] K. E. Aasmundtveit, E. J. Samuelsen, M. Guldstein, C. Steinsland, O. Flornes, C. Fagermo, T. M. Seeberg, L. A. A. Pettersson, O. Inganäs, R. Feidenhans, Macromolecules **33**, 3120 (2000).
[34] H. Liem, P. Etchegoin, K. S. Whitehead, and D. D. C. Bradley, Adv. Funct. Mater. **13**, 66 (2003).
[35] R. D. B. Fraser, J. Chem. Phys. **21**, 1511 (1953).
[36] M. J. Digman, M. Moskovits, and R. W. Stobie, Trans. Faraday Soc. **67**, 3306 (1971).
[37] M. Ariu, D. G. Lidzey, and D. D. C. Bradley, Synth. Met. **111–112**, 607 (2000).
[38] R. M. A. Azzam and N. M. Bashara, J. Opt. Soc. Am. **62**, 1521 (1972).
[39] J. Lee, J. Koh, and R. W. Collins, Opt. Lett. **25**, 1573 (2000).
[40] E. Compain, B. Drevillon, J. Huc, J. Y. Parey, and J. E. Bouree, Thin Solid Films **313–314**, 47 (1998).
[41] M. Schubert, Thin Solid Films **313–314**, 323 (1998).
[42] M. I. Alonso and M. Garriga, Thin Solid Films **455–456**, 455 (2004).
[43] W. A. McGahan, B. Johs, and J. A. Woollam, Thin Solid Films **234**, 443 (1993).
[44] L. A. A. Pettersson, T. Johansson, H. Arwin, F. Carlsson, and O. Inganäs, Synth. Met. **101**, 198 (1999).
[45] L. A. A. Pettersson, S. Ghosh, and O. Inganäs, Org. Electron. **3**, 143 (2002).
[46] SOPRA, *WinElli Manual 3.04* (1997).
[47] R. Azzam and N. Bashara, *Ellipsometry and Polarized Light* (Elsevier, North Holland, 1977).
[48] D. E. Aspnes, J. Opt. Soc. Am. **70**, 1275 (1980).
[49] J. H. Burroughes, D. D. C. Bradley, A. R. Brown, R. N. Marks, K. Mackay, R. H. Friend, P. L. Burns, and A. B. Holmes, Nature (London) **347**, 539 (1990).
[50] H. Sirringhaus, R. J. Wilson, R. H. Friend, M. Inbasekaran, W. Wu, E. P. Woo, M. Grell, and D. D. C. Bradley, Appl. Phys. Lett. **77**, 406 (2000).
[51] G. Heliotis, R. Xia, K. S. Whitehead, G. A. Turnbull, I. D. W. Samuel, and D. D. C. Bradley, Synth. Met. **139**, 727 (2003).
[52] M. Grell, D. Bradley, M. Inbasekaran, and E. P. Woo, Adv. Mater. (Weinheim, Ger.) **9**, 798 (1997).
[53] D. D. C. Bradley, M. Grell, A. Grice, A. R. Tajbakhsh, D. F. O'Brien, and A. Bleyer, Opt. Mater. (Amsterdam, Neth.) **9**, 1 (1998).
[54] M. J. Banach, R. H. Friend, and H. Sirringhaus, Macromolecules **36**, 2838 (2003).
[55] M. R. Drury and D. Bloor, J. Phys. D **23**, 108 (1990).
[56] D. Comoretto, G. Dellepiane, F. Marabelli, J. Cornil, D. A. dos Santos, J. L. Bredas, and D. Moses, Phys. Rev. B **62**, 10173 (2000).
[57] D. Comoretto, F. Marabelli, P. Tognini, A. Stella, J. Cornil, D. A. dos Santos, J. L. Bredas, D. Moses, and G. Dellepiane, Synth. Met. **124**, 53 (2001).
[58] P. Lautenschlager, M. Garriga, L. Vina, and M. Cardona, Phys. Rev. B **36**, 4821 (1987).
[59] G. Heliotis, M. Campoy-Quiles, R. Xia, P. Etchegoin, and D. D. C. Bradley (unpublished).
[60] T. Virgili, D. G. Lidzey, M. Grell, S. Walker, A. Asimakis, and D. D. C. Bradley, Chem. Phys. Lett. **341**, 219 (2001).
[61] J. Cornil, I. Gueli, A. Dkhissi, J. C. Sancho-Garcia, E. Hennebicq, J. P. Calbert, V. Lemaur, D. Beljonne, and J. L. Bredas, J. Chem. Phys. **118**, 6615 (2003).
[62] P. Etchegoin, J. Kircher, M. Cardona, and C. Grein, Phys. Rev. B **45**, 11721 (1992).
[63] A. Mathy, K. Ueberhofen, R. Schenk, H. Gregorius, R. Garay, K. Müllen, and C. Bubeck, Phys. Rev. B **53**, 4367 (1996).
[64] R. F. Bianchi, D. T. Balogh, M. Tinani, R. M. Faria, and E. A. Irene, J. Polym. Sci., Part B: Polym. Phys. **42**, 1033 (2004).
[65] X. H. Wang, M. Grell, P. A. Lane, and D. D. C. Bradley, Synth. Met. **119**, 535 (2001).
[66] T. Kawase, D. J. Pinner, R. H. Friend, and T. Shimoda, Synth. Met. **111–112**, 583 (2000).
[67] A. Sharma, Deepak, S. Kumar, M. Katiyar, A. K. Saxena, A. Ranjan, and R. K. Tiwari, Synth. Met. **138**, 835 (2003).
[68] M. Losurdo, M. M. Ciangregorio, P. Capezzuto, G. Bruno, F. Babudri, D. Colangiuli, G. M. Farinola, and F. Naso, Synth. Met. **138**, 49 (2003).